Yielding to Stress: Recent Developments in Viscoplastic Fluid Mechanics

Neil J. Balmforth,[1] Ian A. Frigaard,[1,2] and Guillaume Ovarlez[3]

[1]Department of Mathematics and [2]Department of Mechanical Engineering, University of British Columbia, Vancouver V6T 1Z2, Canada; email: njb@math.ubc.ca

[3]Laboratoire Navier (UMR 8205), CNRS, ENPC, IFSTTAR, Université Paris-Est F-77420 Marne-la-Vallée, France

Annu. Rev. Fluid Mech. 2014. 46:121–46

First published online as a Review in Advance on August 14, 2013

The *Annual Review of Fluid Mechanics* is online at fluid.annualreviews.org

This article's doi: 10.1146/annurev-fluid-010313-141424

Keywords

viscoplastic fluids, yield stress

Abstract

The archetypal feature of a viscoplastic fluid is its yield stress: If the material is not sufficiently stressed, it behaves like a solid, but once the yield stress is exceeded, the material flows like a fluid. Such behavior characterizes materials common in industries such as petroleum and chemical processing, cosmetics, and food processing and in geophysical fluid dynamics. The most common idealization of a viscoplastic fluid is the Bingham model, which has been widely used to rationalize experimental data, even though it is a crude oversimplification of true rheological behavior. The popularity of the model is in its apparent simplicity. Despite this, the sudden transition between solid-like behavior and flow introduces significant complications into the dynamics, which, as a result, has resisted much analysis. Over recent decades, theoretical developments, both analytical and computational, have provided a better understanding of the effect of the yield stress. Simultaneously, greater insight into the material behavior of real fluids has been afforded by advances in rheometry. These developments have primed us for a better understanding of the various applications in the natural and engineering sciences.

1. INTRODUCTION

Every day we deal with many materials that can be described as viscoplastic fluids: We squeeze toothpaste from tubes, spread butter and jam over toast, apply cosmetic creams to skin, clean mud from boots, and dispose of unpleasant waste products and bodily secretions. A great many industrial processes involve viscoplastic fluids, ranging from the creation of chocolate confections to the pulp suspensions of paper making and the concrete used for construction. So too do environmental hazards such as mud and lava flows, landslides, and avalanches. Biological materials such as mucus can be viscoplastic, making relevant problems in physiology, biolocomotion, and beyond. The common feature of all these materials is that they flow when pushed sufficiently strongly; when left alone, they either simply sit there or maneuver on a much longer timescale. In other words, they combine solid-like behavior at low stresses with a fluid-like response at high stress.

A convenient way to describe the switch from fluid to solid behavior is in terms of the yield stress required to trigger the transition, which is, perhaps surprisingly, taken to be a sharply defined value rather than some mean measure of a characteristic range. The fluid dynamicist seems most comfortable with the description of these materials as viscoplastic fluids. The experimentalist more frequently prefers the terminology yield-stress fluids. The jamming or glassy materials of the physicist are closely related, and the engineer has several looser descriptions, including pastes, muds, and slurries. In any event, such materials are the focus of this review; some examples are shown in **Figure 1**.

A simple cartoon of non-Newtonian fluid behavior is often afforded by plotting the flow curve of a material, in which one records a measure of stress against a measure of the rate of deformation. The resulting curve reflects the assumption that the instantaneous stress of the material is determined purely by the local deformation rate or, equivalently, that one can define an effective viscosity. This model of constitutive behavior is usually referred to as the generalized Newtonian fluid and, in view of its simplicity and ease of construction by rheometers, has received much attention in engineering settings.

A simple extension of the generalized Newtonian model is to allow the flow curve to have jumps in gradient, implying switches in viscosity. A switch at a zero deformation rate furnishes the simplest type of yield-stress fluid models, of which the Bingham model is the most extreme. For this model, the deformation rates vanish until the yield stress is reached, whereafter the fluid flows with a constant plastic viscosity. In simple, unidirectional shear, one expresses this law by relating the stress, τ, to the shear rate, $\dot{\gamma}$, by

$$\dot{\gamma} = 0 \quad \text{if} \quad \tau < \tau_Y, \quad \text{and} \quad \tau = \tau_Y + \mu\dot{\gamma} \quad \text{otherwise},$$

where τ_Y and μ are the yield stress and plastic viscosity, respectively. More generally, one poses the three-dimensional (3D), tensorial formulation

$$\dot{\gamma}_{ij} = 0 \quad \text{if} \quad \tau < \tau_Y, \quad \text{and} \quad \tau_{ij} = \tau_Y \frac{\dot{\gamma}_{ij}}{\dot{\gamma}} + \mu\dot{\gamma}_{ij} \quad \text{otherwise}, \tag{1}$$

where τ_{ij} is the deviatoric stress tensor, $\dot{\gamma}_{ij} \equiv \partial u_i/\partial x_j + \partial u_j/\partial x_i$ represents the strain-rate tensor, and τ and $\dot{\gamma}$ are now the second invariants,

$$\tau \equiv \sqrt{\sum_{i,j} \frac{1}{2}\tau_{ij}^2}, \quad \dot{\gamma} \equiv \sqrt{\sum_{i,j} \frac{1}{2}\dot{\gamma}_{ij}^2}. \tag{2}$$

In technical detail, the Bingham model assumes that the fluid's material structure is isotropic, there are no normal stress differences, and there is no account of either elasticity or temporal

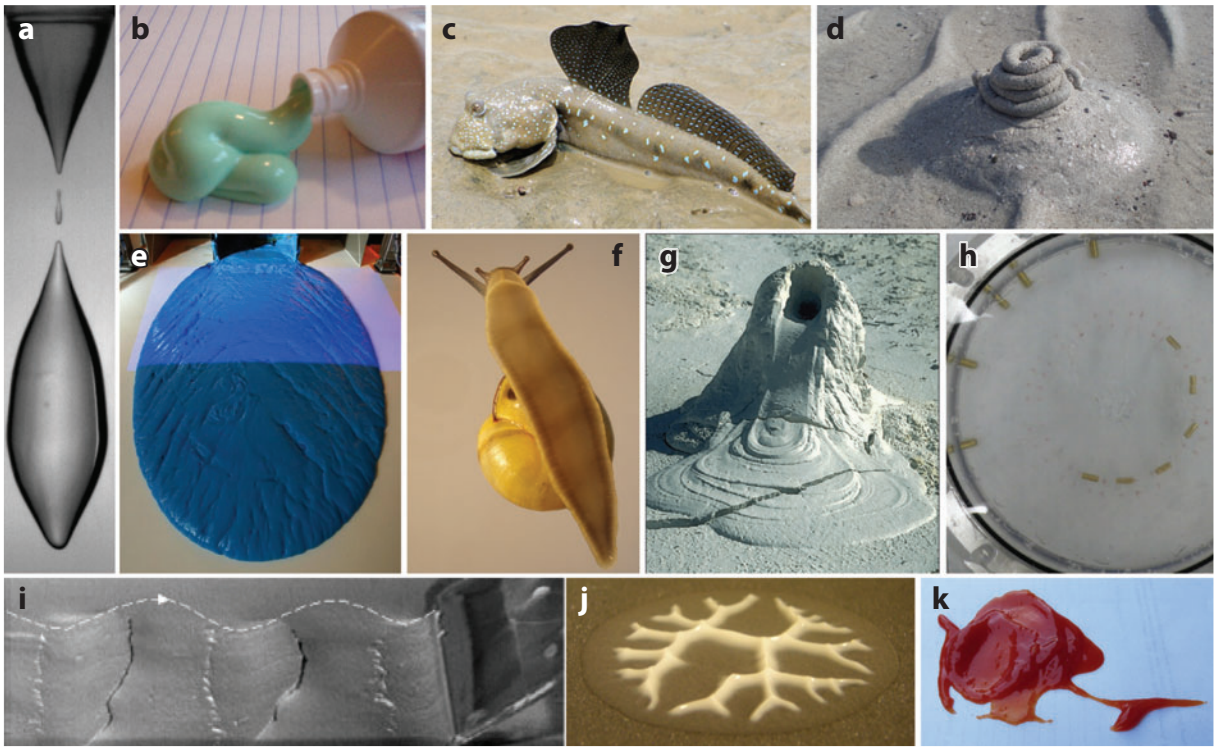

Figure 1

Some traditional viscoplastic materials in nontraditional flow configurations, and some nontraditional viscoplastic fluid flows (plus pertinent references). (*a*) Pinch-off and drips of Carbopol (German & Bertola 2010a,b). (*b*) A collapsed extrusion of toothpaste (Kamrin & Mahadevan 2012). (*c*) A mudskipper moving over mud (Pegler & Balmforth 2013). Photograph courtesy of Nick Baker. (*d*) A mud mound composed from a collapsed helical tube extruded by a sandworm via peristaltic action (Rahmani et al. 2011) amid ripples on the beach. (*e*) A dambreak of blue-colored Carbopol on an incline (Cochard & Ancey 2008). Photograph courtesy of C. Ancey. (*f*) The underside of a snail's foot; the mucus layer plays a key role in its adhesive locomotion (Denny 1981). (*g*) A mud volcano. Photograph courtesy of the USGS. (*h*) Particle fractionization in Carbopol (Madani et al. 2010). (*i*) A mud washboard (Hewitt & Balmforth 2012). (*j*) Viscoplastic Saffman-Taylor fingers (Barral et al. 2010). (*k*) Ketchup splatter (Luu & Forterre 2009).

relaxation. The yield criterion, $\tau \to \tau_Y$, is based on a single invariant of the stress tensor and is the von Mises criterion of plasticity theory (see Section 3.6) (Prager & Hodge 1951).

The simplicity of the Bingham law has given this model a special status in viscoplastic fluid mechanics, yet there is no doubt that it fails to quantitatively describe any real material (except, perhaps, over a limited range of stresses). A popular variant is the Herschel-Bulkley model, which includes a rate-dependent viscosity in the form of a power law, replacing the second part of Equation 1 with

$$\tau_{ij} = \tau_Y \frac{\dot{\gamma}_{ij}}{\dot{\gamma}} + K\dot{\gamma}^{n-1}\dot{\gamma}_{ij}, \quad \text{if } \tau \geq \tau_Y; \tag{3}$$

the consistency is K, and the index n allows for a viscosity that decreases with the shear rate if $n < 1$ (shear thinning) or increases with $\dot{\gamma}$ if $n > 1$ (shear thickening). The Herschel-Bulkley law is more realistic because the material structure that resists deformation and leads to the yield stress is typically not completely destroyed at $\tau = \tau_Y$. Instead, the structure persists postyield and renders the viscosity shear-rate dependent. In other words, viscoplastic fluids usually exhibit both a yield stress and a nonlinear viscosity. Efforts to establish firmer connections of constitutive

laws such as the Herschel-Bulkley model with microscopic dynamics are reviewed in Section 3.4. The stress–strain rate relation for a real viscoplastic fluid is illustrated in **Figure 2*a***. This fluid, a Carbopol gel, is described relatively well by the Herschel-Bulkley model (at least in steady shear), as illustrated by the fit also included in the plot and discussed in more detail in Section 3.2.

The most dramatic feature of a viscoplastic fluid is the yield stress: From both a physical and mathematical perspective, this threshold effects a fundamental change to the fluid mechanics of the problem. However, a rate-dependent viscosity effects little qualitative change to the mathematical and physical structure. For this reason, we do not review the literature that generalizes Newtonian fluid problems by making the viscosity nonlinear but focus on yield-stress effects. In Section 2, we review the main recent theoretical developments, both analytical and computational, which have allowed for a better understanding of such effects. We provide a counterpoint in Section 3 by discussing the new insights into the behavior of real viscoplastic fluids that have been provided by recent advances in rheometry. Finally, Section 4 summarizes examples in which these developments have primed us for a better understanding of applications in the natural and engineering sciences.

Augmented Lagrangian methods: methods that allow one to perform viscoplastic flow computations using the variational formulation of the Navier-Stokes equations and an optimization algorithm

Viscosity regularization: methodology that replaces the singular effective viscosity of an idealized yield-stress model with a large, but finite viscosity

2. MODELING WITH IDEALIZED YIELD-STRESS FLUIDS

2.1. Computing Flows of Viscoplastic Fluids

The key computational challenge with viscoplastic fluid flows is to correctly reproduce the rigid structure of the plug regions, where the stress is below the yield stress, and to track the yield surfaces that separate plugs from yielded regions (see **Figure 2*d*** for an example of a plug in a Couette cell). Yield surfaces are not material surfaces, and we must pose a free boundary problem in which the stress dictates the position of the free boundary. Computational approaches were proposed in the 1980s (e.g., Glowinski et al. 1981) and have since been used to compute increasingly complicated flows (e.g., Dimakopoulos et al. 2013, Hormozi et al. 2011, Vinay et al. 2006, Vola et al. 2004, Yu & Wachs 2007).

Two main methods have developed. Augmented Lagrangian methods are based on the variational formulation of the Navier-Stokes equations and determine the flow solution via an optimization algorithm. Because of the form of yield-stress constitutive laws, the optimization is complicated by the nondifferentiability of the dissipation-rate functional at the yield surface. This technical difficulty is avoided by introducing a related saddle-point problem, which is solved iteratively (see Glowinski & Wachs 2011 for a detailed review).

The second methodology retains the classical formulation and regularizes the constitutive law: For an idealized yield-stress fluid, the effective viscosity becomes infinite at the yield surface and within a plug. Regularization replaces this singularity by a large, but finite viscosity, thereby eliminating any yield surfaces and replacing the plugs with very viscous fluid. Frigaard & Nouar (2005) provide a recent review of popular regularization schemes.

Both augmented Lagrangian and regularization methods have been implemented in finite-element and finite-volume discretizations. Augmented Lagrangian schemes are generally slower than codes with viscosity regularizations and are more complex to implement. Regularization typically furnishes smoother solutions for the velocity field, parameterized by a regularization parameter $\epsilon \ll 1$ such that the velocity solution of the exact yield-stress model is recovered when $\epsilon \to 0$. This smoothness allows the application of more sophisticated flow solvers and leads to faster computations. Regularization can be implemented within many commercial computational fluid dynamics codes via a user-defined viscosity function, exploiting built-in functions for meshing, numerical integration, and so forth, which is a practical advantage. However, as $\epsilon \to 0$, the regularized solution becomes progressively more difficult to compute. In practice, one chooses

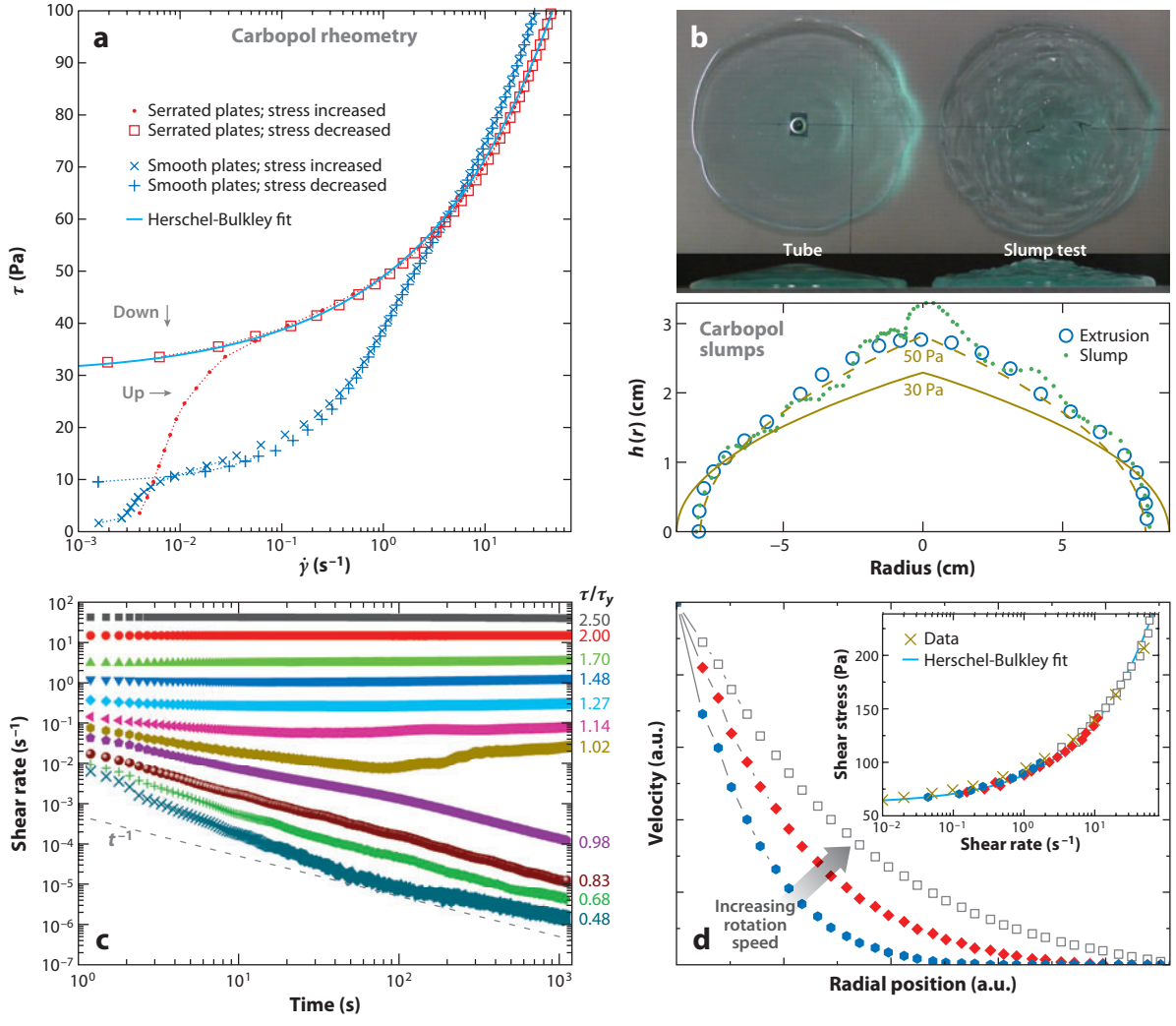

Figure 2

Carbopol flow curves and slumps. (*a*) Flow curves from a plate-plate rheometer. The red symbols show the curve for a test with serrated plates in which the stress was increased (at 0.5 Pa/s; *dots*) and then decreased (*squares*). The light blue line is a Herschel-Bulkley fit with $\tau_Y = 30$ Pa, $n = 0.34$, and $K = 19$ Pa/s. Below the yield stress on the up curve, data correspond to the elastic straining of the material in its solid-like regime. The blue crosses show a flow curve for the same material, but using smooth plates, to indicate the effect of slip. (*b*) Photographs of the final domes resulting from a fixed-flux extrusion from a tube (*left*) and a slump test (*right*) on a horizontal plexiglass plate with a roughened surface. Roughly the same volume of Carbopol was poured out from a beaker in the slump test. The plots show depth profiles (*blue circles* show the extrusion, and *green dots* show the slump). The dark yellow solid (dashed) curve shows the thin-film prediction given in Equations 4 and 5, assuming a yield stress of 30 Pa (50 Pa). (*c*) Shear rate against time during creep tests performed in a Couette geometry at the scaled applied stresses, τ/τ_Y, indicated. The gray dashed line shows the trend t^{-1}. For $\tau = 1.02\tau_Y$, we note the solid-like creep flow at short times, followed by the eventual onset of steady flow. (*d*) Dimensionless velocity profiles measured locally in the gap of a 1.9-cm-wide gap Couette cell with magnetic resonance imaging techniques (see Section 3.3). Profiles from left to right correspond to increasing rotation speed of the inner cylinder (data from Coussot et al. 2009). At the lower velocity, flow is localized near the inner cylinder, and there is a plug near the outer cylinder. As the rotation increases in speed, the plug becomes thinner; all the material flows at the highest rotation speed. (*Inset*) The flow curve reconstructed from the velocity profiles (see Section 3.3). The dark yellow crosses are data measured with standard rheometry, in a cone-and-plate geometry, and the light blue line shows a Herschel-Bulkley fit. The rheometry and slumps in panels *a* and *b* use the same Carbopol solution; different samples are used in panels *c* and *d*.

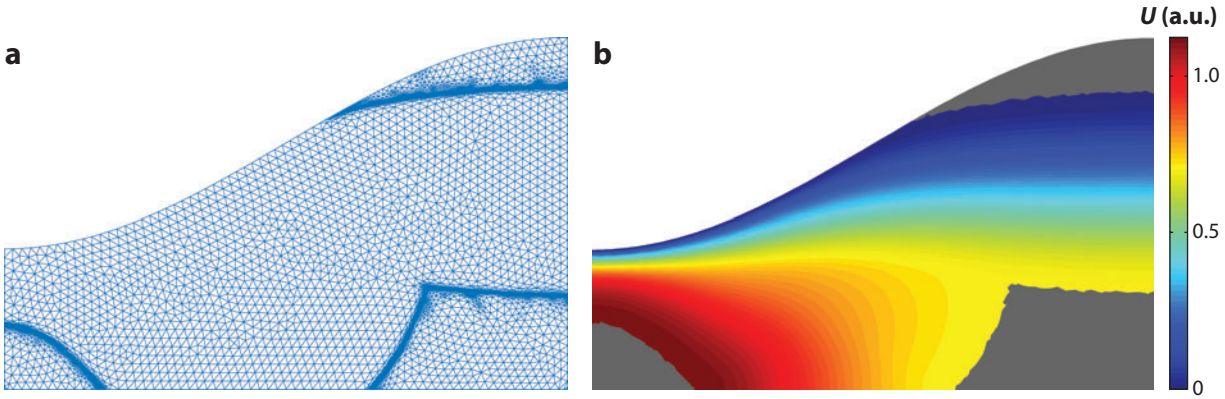

Figure 3

Numerical solution for flow down a wavy-walled channel, computed with an augmented Lagrangian scheme [using the code Rheolef (Roquet & Saramito 2003), performed by A. Roustaei]. (*a*) The mesh of the finite-element discretization used (9,460 elements, with a high density surrounding the yield surfaces). (*b*) Speed as a density on the (x, y) plane, with the plugs shaded gray. One-quarter of the periodic channel is shown, with the solution symmetrical about $y = 0$ and $x = 0$. The Bingham number, $B = \tau_y H/\mu U = 5$, is based on the mean velocity U and the half width of the narrowest part of the channel H.

a small fixed ϵ, and it is essential to check that this value is sufficiently small to ensure adequate convergence of the velocity field. Less satisfactorily, no theory exists to guarantee that the stress field also converges to the correct solution. Thus, one cannot conclude that the regularized plug regions (identified using a contour of constant stress or strain rate) converge to the true ones. Nevertheless, numerical solutions have converged correctly in a few nontrivial flows with known yield surfaces (e.g., Burgos et al. 1999).

Pragmatically, the choice between augmented Lagrangian and regularization is related to whether one needs to determine the position of the yield surface, or whether a reasonable approximation to the velocity field is sufficient. Explorations of the plastic limit (see Section 2.2) provide an important class of problems in which the accurate determination of the yield surface is required. Some form of mesh adaptivity in combination with an augmented Lagrangian scheme is then usually desired, as implemented, for example, in the free software Rheolef (Roquet & Saramito 2003) (see **Figure 3**, which shows a numerical solution for flow down a wavy-walled channel computed using this scheme).

A potentially more elegant approach is to compute only the yielded flow solution while tracking the yield surfaces explicitly (e.g., Beris et al. 1985, Szabo & Hassager 1992). Unfortunately, the existing implementations are restrictive because they take advantage of known plug geometry, and it is unclear how to generalize these schemes to make them more flexible. Other recent developments include the use of meshless schemes, such as lattice Boltzmann (Derksen 2013, Vikansky 2008).

2.2. Variational Methods and the Plastic Limit

The variational formulation of viscoplastic flow problems has applications beyond numerical algorithms (Section 2.1). Slow, steady flows of viscoplastic fluids satisfy two variational principles (Duvaut & Lions 1976, Prager 1954): a rate of strain minimization and a stress maximization principle. These variational principles can provide bounds on the drag on rigid objects moving through viscoplastic fluid (e.g., Adachi & Yoshioka 1973) and identify how quantities such as the

dissipation and flow rates vary with problem parameters (e.g., rheological constants, imposed pressure gradient) (Duvaut & Lions 1976). They are particularly useful in exploring the plastic limit (e.g., Duvaut & Lions 1976, Mossolov & Miasnikov 1965). Recent applications include the arrest of motion of suspended bubbles and particles (see Section 4.3) (Dubash & Frigaard 2004, Putz & Frigaard 2010, Tokpavi et al. 2008).

Plastic limit: point at which the imposed stresses fall beneath the yield stress everywhere and flow ceases

When the critical limit required for sustained flow is not exceeded, only transient motion can be triggered by an initial disturbance. In contrast to viscous fluids, the yield stress brings flow in fixed domains to rest in finite time. This has been recently illustrated by Muravleva et al. (2010) for 1D duct flows and by Zhang et al. (2006) for thermal convection. The ideas have even been applied in image processing (Frigaard et al. 2003), in which there are mathematical analogies with nonlinear filtering. Curiously, theory for viscoplastic films with a free surface (see Sections 2.3 and 4.2) suggests infinite stopping times (Matson & Hogg 2007); this may be an artifact of the thin-film approximation.

Plastic limit analysis for a yield-stress fluid is closely connected to classical plasticity theory (Prager & Hodge 1951). Despite this, plasticity solutions have rarely been used in viscoplastic fluid mechanics. Examples include plastic flow around sedimenting objects (Beris et al. 1985, Putz & Frigaard 2010, Tokpavi et al. 2008) and in slumps on inclined planes (see Section 4.2) (Dubash et al. 2008). More curious is the dearth of viscoplastic flow solutions corresponding to some of the classical problems of solid mechanics. The bending and buckling of beams have recently been studied for viscoplastic fluids (Balmforth & Hewitt 2013, Kamrin & Mahadevan 2012). However, the indentation of a punch into a plastic half space has never received any viscoplastic consideration, despite the classical solutions of Prandtl and Hill (see Prager & Hodge 1951) and a number of applications, including locomotion and imprinting patterns on mud (see Section 4.4 and **Figure 1**) (Hewitt & Balmforth 2012).

2.3. Thin-Film and Lubrication Theories

The asymptotic analysis of thin viscoplastic films, or viscoplastic lubrication theory, dates back to the 1950s and even appears in classical texts (Pinkus & Sternlicht 1964). Objections to this theory emerged in the 1980s with the observation that lubrication analyses were apparently inconsistent: The "lubrication paradox" of Lipscomb & Denn (1984) highlighted how the theory predicted plug regions that were apparently below the yield stress, even though the velocity field there was not fully rigid. This inconsistency caused many workers to consider regularized viscoplastic constitutive models and explore unphysical distinguished limits. Such diversions ultimately prove unnecessary because the paradox can be resolved by recognizing that the lubrication theory is the leading-order term of an asymptotic expansion; an exploration of higher-order terms demonstrates that the problematic plugs are actually slightly above the yield stress, allowing for their deformation (Putz et al. 2009, Walton & Bittleston 1991). The regions have been termed pseudoplugs to emphasize their nature, with their borders referred to as fake yield surfaces. There is therefore no lubrication paradox.

The occurrence of pseudoplugs in slowly varying geometries leads to two secondary questions. First, can truly rigid plugs be embedded within them? True plugs potentially surround points of symmetry at which the strain-rate invariant must vanish; this can be verified, and the extent of the plugs determined, by considering the force balance on these regions. In this fashion, Walton & Bittleston (1991), Szabo & Hassager (1992), and Putz et al. (2009) built true plugs at the cores of pseudoplugs in flow between eccentric cylinders and down a wavy-walled channel. The second question is whether the pseudoplugs develop into true plugs when their weak spatial variations become sufficiently small. This has been confirmed by Szabo & Hassager (1992) and Frigaard &

Ryan (2004) in two particular geometries. Both questions demand a more elaborate asymptotic analysis than leading-order lubrication theory.

Other recent work has explored viscoplastic film dynamics in a wider range of configurations and applications. The squeeze flow problem, which originally motivated Lipscomb & Denn's lubrication paradox, is well studied (Engmann et al. 2005, Sherwood & Durban 1998), although the true plugs that must lie at the core of this flow have been constructed only numerically (Karapetsas & Tsamopoulos 2006); a detailed asymptotic analysis has not been tried, nor have the connections with classical plasticity solutions been fully exploited (Prager & Hodge 1951). Shallow viscoplastic flow over an inclined plane, the analog of the classical viscous gravity current problem, is discussed further in Section 4.2; other free-surface problems with popular viscous counterparts include surface-tension-driven viscoplastic fingering (de Bruyn et al. 2002) and the pinch-off, bending, and buckling of free viscoplastic sheets and filaments (Balmforth et al. 2010; Balmforth & Hewitt 2013; German & Bertola 2010a,b; Kamrin & Mahadevan 2012; Rahmani et al. 2011).

2.4. Hydrodynamic Stability of Viscoplastic Fluids

Advances in viscoplastic stability theory are mostly relatively recent, providing parallel treatments of some of the classical hydrodynamic instabilities (the earlier literature is reviewed in Georgievskii 2011). For nearly all flows studied to date, the effect of the yield stress is to enhance stability.

A critical facet of viscoplastic stability problems is the role played by the rigid plugs of the base state. Fully yielded base flows present no particular mathematical difficulty to conventional stability analysis, and the critical conditions for instability usually vary smoothly with yield stress upon proceeding away from the Newtonian limit, even if plugs subsequently appear in the base state. Taylor-Couette flow provides such an example (Landry et al. 2006, Peng & Zhu 2004).

By contrast, fully unyielded base states are significantly different, becoming unconditionally linearly stable because an infinitesimal perturbation cannot raise the equilibrium stress above the yield value. The viscoplastic Rayleigh-Bénard problem is a classical example (Zhang et al. 2006): the critical Rayleigh number for the onset of convection becomes infinite with the addition of any yield stress. This striking result is in clear conflict with the classical threshold, which cannot be recovered by taking the Newtonian limit; in other words, the combined limit of vanishing amplitude and yield stress must be treated with care. Physically, the fluid simply cannot remain rigid when the amplitude of the stress perturbation is of the order of the yield stress.

Despite the dramatic change in the linear stability of the conducting state, one does not expect vigorous convection to be much affected by a relatively small yield stress. Thus, convective solutions with sufficient finite amplitude ought to survive the introduction of the yield stress. However, these solutions appear in the Newtonian problem when the conducting state loses stability at the classical threshold; how can they therefore be created when the yield stress shifts the point of linear instability to infinite Rayleigh number? As outlined by Zhang et al. (2006) and Balmforth & Rust (2009), the supercritical onset of Newtonian convection is replaced by a rather different bifurcation structure: Unstable convective modes with weak amplitude appear first by bifurcating subcritically from infinite Rayleigh number; as one traces these solutions back to lower temperature gradients, their amplitude strengthens until, closer to the Newtonian threshold, the solution branch turns back to higher Rayleigh numbers, becoming stable and creating the more vigorous convecting states. Thus, convection is delayed to higher Rayleigh numbers by the yield stress and requires a finite-amplitude disturbance to be initiated. As the yield stress becomes small, so too do the shift in onset and the magnitude of the kick needed to convect, rationalizing how the viscoplastic problem converges to its Newtonian counterpart.

For partially yielded base flows, the linear stability equations are posed only over the yielded flow domain, with boundary conditions imposed at the perturbed yield surfaces (Frigaard et al. 1994). How dramatically the yield stress affects the linear stability then depends on whether the plug immobilizes fluid over a region that is critical to the instability mechanism or whether the plug effects a fundamental change to the form of the imposed boundary conditions. For example, linear Newtonian instabilities associated with free-surface or interfacial motion are completely eliminated if there is an adjacent plug (see Section 4.1) (Balmforth & Liu 2004, Frigaard 2001); the surface or interface can no longer be perturbed to trigger linear instability, and finite-amplitude instability is instead needed for instability, as for convection. In Poiseuille flows, the central plug acts like a solid wall, dividing the yielded flow into two sections, each with a velocity profile that is equivalent to a mixed Poiseuille-Couette flow; the Couette component stabilizes the viscous modes (Métivier et al. 2005, Nouar et al. 2007). Here the plug is responsible for imposing boundary conditions on the perturbation that are quite different from the usual conditions in an unyielded shear flow; these conditions directly affect the linear stability problem by stabilizing the viscous modes. Again, the Newtonian limit conflicts with classical stability results because the central plug, no matter how thin, cannot be broken.

In situations in which finite-amplitude instability may arise, one must advance beyond linear theory with, for example, energy stability methods or weakly nonlinear theory. Energy methods have been used to place bounds on instability in viscoplastic shear flows (see Nouar & Frigaard 2001) and convection (Zhang et al. 2006), and weakly nonlinear theory applied to Rayleigh-Bénard-Poiseuille flow (i.e., thermal convection in a channel flow) (Métivier et al. 2010). However, the application of these methods remains limited. In particular, in energy stability theory, the role of the yield stress is relatively unexplored: Because the unyielded state is assumed rigid, the stress over a plug is formally indeterminate in the base flow (Prager & Hodge 1951). It is equally admissible to assume that the plug is held close to the yield stress, or at stresses significantly below that critical value. Any prestress built into the base flow renders that state significantly less stable, with the plugs breaking up with relatively weak perturbations [the rationalization of viscoplastic roll waves proposed by Balmforth & Liu (2004)]. In general, to address such issues, one must pose the stability analysis as a variational problem and build in a measure of the prestress. Alternatively, one can abandon the idealized yield-stress model in favor of a constitutive law that accounts for subyield deformation and uniquely determines the stress state (Saramito 2009, Thompson & de Souza Mendes 2012).

3. REAL CONSTITUTIVE BEHAVIOR

3.1. De-Mythifying the Yield-Stress Myth

Approximately 30 years ago, Barnes & Walters (1985) published their controversial article on the "yield-stress myth," questioning whether a yield stress truly existed, or if there was always highly viscous flow at low shear rates; the measured yield stresses were claimed to be merely the thresholds at which the viscosity fell abruptly (Barnes 1999). Recent advances in rheometry offer new insight into this issue. Important results are that (*a*) flows observed at low stresses are not always steady, and (*b*) flow complexity (shear bands, wall slip) can lead to erroneous interpretation of macroscopic data.

The simplest experiment to see whether a material flows or not consists of applying a constant homogeneous stress and then measuring the resulting shear-rate variation in time. Careful examination of this response shows that, for durations as long as days, only unsteady flows occur at the lower stresses, characterized by very low shear rates that keep decreasing in time (see **Figure 2*c***)

and an apparent viscosity that continually increases with time (Caton & Baravian 2008, Coussot et al. 2002a, Moller et al. 2009). This has been observed with materials similar to those analyzed by Barnes (1999), such as Carbopol gels (Coussot et al. 2006, Divoux et al. 2011, Moller et al. 2009), muds (Coussot et al. 2002a, 2006), and mayonnaise (Caton & Baravian 2008, Da Cruz et al. 2002). The phenomenon is particularly spectacular in thixotropic fluids (see Section 3.5). It thus seems that the Barnes & Walters viscosity data at low stresses were not steady state (Moller et al. 2009), which was probably hard to detect at the time. In the creep regime, the shear rate for simple yield-stress fluids follows the trend $\dot{\gamma} \propto t^{-n}$, with n varying between 0.6 and 1 (see **Figure 2*c***), which is reminiscent of the primary creep observed in solids (Caton & Baravian 2008, Divoux et al. 2011).

Static yield stress ($\tau_{y,s}$): the stress above which unyielded fluid begins to flow

Dynamic yield stress ($\tau_{y,d}$): the stress below which yielded fluid stops flowing

Nevertheless, a true yield stress remains hard to determine: There exists a range of stresses in which this creep regime is followed by a series of complex events (wall slip even with rough boundaries, transient shear banding) during which the flow accelerates macroscopically and ultimately becomes steady and homogeneous (see Section 3.3) (Caton & Baravian 2008, Divoux et al. 2011). The time to reach steady flow can be as long as days and seems to diverge at a critical stress. This divergence would rigorously define a yield stress (Caton & Baravian 2008, Divoux et al. 2011), but its characterization relies on the patience of the experimentalist. More pragmatically, the relevant yield stress to consider in a problem may be dictated by the timescale of the problem itself. Note that these complicating features mostly characterize start-up flows (Divoux et al. 2011) and are not apparently observed when decreasing the shear stress on a steady flow (Ovarlez et al. 2013). Consistently, the critical stress above which flows can be initiated may be slightly higher than the critical stress for which steady flows are allowed in most materials (i.e., the static yield stress exceeds the dynamic yield stress) (Chaudhuri et al. 2012, Divoux et al. 2011, Ovarlez et al. 2013).

3.2. Prototypical Viscoplastic Fluids

In steady-state shear flow, several materials have behavior close to the paradigm of the Herschel-Bulkley model: microgel suspensions (Coussot et al. 2009) (**Figure 2*a***), colloidal glasses (Besseling et al. 2007), and foams and concentrated emulsions (Ovarlez et al. 2013) (see also Section 3.3). Microgels are deformable particles made from polymeric gel, with a notable example being Carbopol (Piau 2007). Other microgels can be produced with a better-characterized structure (Seth et al. 2011). Colloidal glasses are dense suspensions of Brownian particles that form a glassy structure above a critical volume fraction (Besseling et al. 2007, Mewis & Wagner 2012). They benefit from a solid theoretical framework, making them strong candidates for understanding the link between Herschel-Bulkley behavior and microscale dynamics, but they cannot be produced in large amounts and are thus limited to small-scale studies (rheometry, microfluidics). Aqueous foams are dense assemblies of bubbles in aqueous solution. Their drawback is the rapid evolution in time due to drainage and bubble coarsening (Cohen-Addad et al. 2013). Nevertheless, they can be usefully arranged into quasi-2D flows, in which individual bubbles can be tracked (Katgert et al. 2010) and the local stress field extracted from the bubble shape (Dollet & Graner 2007). Concentrated emulsions are assemblies of liquid droplets in an immiscible liquid. They pose less stability problems than do foams and can be made transparent, which makes them a possible alternative to Carbopol gels. Importantly, these emulsions may be less elastic and feature lower normal stress differences than Carbopol gels.

Many of these prototypical fluids have been used for the viscoplastic counterparts of classical viscous flow experiments, as described elsewhere in this review. Most experiments have been performed with Carbopol gels because of their low cost, ease of preparation and disposal,

reproducibility, and transparency. Their transparency allows the use of seeding and optical techniques to track flow fields and determine yield surfaces (e.g., Ancey et al. 2012, Putz et al. 2008, Tokpavi et al. 2009b). Nevertheless, these materials also deviate from the behavior of an idealized yield-stress fluid: They display normal stress differences (Piau 2007), which can play a role, for example, in flows around obstacles (Dollet & Graner 2007, Putz et al. 2008, Tokpavi et al. 2009b) and in the determination of the yield surface (Cheddadi et al. 2012). They can be significantly elastic above the yield stress (Benmouffok-Benbelkacem et al. 2010, Piau 2007), which has to be accounted for in flows such as impacts on surfaces (Luu & Forterre 2009). Such features have motivated the development of elastoviscoplastic models and other generalizations of the Herschel-Bulkley law (Saramito 2009).

Shear banding: the coexistence of a liquid-like flow and a solid-like region in a homogeneous stress field

3.3. Macroscopic Versus Local Behavior

An important recent experimental development has been the combination of flow visualization with standard rheometry. The velocity field can be obtained optically in 2D systems (Katgert et al. 2010), transparent fluids (Besseling et al. 2010), or weakly scattering materials (Salmon et al. 2003) and by ultrasonic Doppler velocimetry (Manneville 2008) and magnetic resonance imaging techniques (Bonn et al. 2008) in many other systems (see **Figure 2*d***). Information on local material composition (Fall et al. 2010, Ovarlez et al. 2013) or structure (Besseling et al. 2007, Masschaele et al. 2009, Oppong & de Bruyn 2011, Pignon et al. 1998) can also be obtained.

The combination of macroscopic and local information has given better insight into the true material behavior in cases in which the assumptions underlying rheometry (no-slip, flow and material homogeneity) are violated. Much new behavior (Bonn et al. 2008, Manneville 2008, Mansard & Colin 2012, Ovarlez et al. 2009, Schall & van Hecke 2010) has been discovered, most of which could not have been found with blind rheometry alone. For example, start-up flows of Carbopol gels have been found to be quite complex at the local scale: Divoux et al. (2011) have observed full slip, even with rough boundaries, followed by long-lived, transient, shear-banded flows that eventually become steady and homogeneous; this is yet to be explained. In suspensions of rigid particles, stationary shear bands have been observed for stresses close to the yield stress; they are attributed either to flow-induced concentration inhomogeneities (Besseling et al. 2010, Fall et al. 2010) or to competition between sedimentation and shear-induced resuspension (Fall et al. 2009). Steady-state shear bands have also been observed in thixotropic materials (Coussot et al. 2002b, Moller et al. 2008, Ovarlez et al. 2009; Section 3.5), reflecting the competition between aging and shear-induced rejuvenation (Coussot et al. 2002b, Moller et al. 2006).

In geometries in which the shear stress is fully determined by a force balance, the flow curve can be extracted directly from the observed shear-rate profile (**Figure 2*d***) (Mansard & Colin 2012, Ovarlez et al. 2013). Unexpectedly, in some cases, different local flow curves are needed for different boundary conditions (Goyon et al. 2008, Katgert et al. 2010). These observations have been rationalized using nonlocal constitutive equations (Goyon et al. 2008, Mansard & Colin 2012). Such nonlocal effects seem to be restricted to systems of small size (as compared with the size of the material mesoscopic elements). Indeed, in wide-enough geometries, if the complexities of start-up flow are carefully avoided, the Herschel-Bulkley law accounts for the flows of many yield-stress fluids, such as Carbopol gels, foams, and concentrated emulsions (see Section 3.2) (Goyon et al. 2008, Ovarlez et al. 2013). Furthermore, the law is consistent with the observed macroscopic behavior, thus validating standard rheometry under these conditions (**Figure 2*d***). Thus, simple rheometry can certainly be used to establish flow curves and characterize material behavior in many practical situations.

3.4. The Microscopic Connection

Thixotropic material: material with a microstructure that slowly builds up when the fluid is left to rest but is broken down under shear; structuration, also known as healing or aging, is the increase in microstructure, and destructuration, or rejuvenation, is its break-up by shear

For years, viscoplastic fluid mechanics has largely rested on an empirical foundation: The Bingham and Herschel-Bulkley models, and all their modifications, were essentially fits to rheometric flow curves in simple shear. However, the link between microscopic structure and macroscopic flow properties has now begun to emerge.

The existence of a yield stress is well understood for suspensions of attractive colloids (Mewis & Wagner 2012), foams, and concentrated emulsions (Cohen-Addad et al. 2013). The case of dense suspensions of repulsive colloids is more complex: Their yield stress emerges when their structure cannot relax anymore (Besseling et al. 2007, Mewis & Wagner 2012); modeling then involves concepts from glass theory (Brader et al. 2009) and jamming (Liu & Nagel 2001). Colloidal suspensions with attractive interactions have a yield stress when a percolated network of stuck particles forms, and flow requires the breakage of some links; the yield stress can be computed using the interaction forces and microstructure (Mewis & Wagner 2012). At rest, foams are in a metastable state, which minimizes the total surface area of air/liquid interfaces; when sheared, interfaces are progressively deformed and store elastic interfacial energy. At a critical deformation, the configuration loses stability, and plastic rearrangements take place (Cohen-Addad et al. 2013); the equivalent yield stress is a function of surface tension, bubble size, liquid fraction, and microstructure. Interestingly, in real foams, there is also gas exchange between neighboring bubbles, leading to coarsening and internal rearrangements; any small applied stress introduces a distortion in the spatial distribution of these rearrangements, leading to irreversible deformation in the direction of shear (Cohen-Addad et al. 2004), which explains the existence of slow viscous flow below the yield stress in foams. No generic description of the subyield regime exists for other materials (see Section 3.1).

The origin of the nonlinear plastic viscosity is still under debate. A basic explanation can be given for foams and concentrated emulsions: Dissipation in the interstitial Newtonian fluid between undeformed bubbles and droplets would suggest a constant viscosity at the macroscopic scale. However, the interfaces are deformed under shear, and the average thickness of the films in which dissipation occurs then depends on the viscous stress acting on the interfaces (i.e., on $\dot{\gamma}$). The interplay between the local viscous flow and the material microstructure suggests a power-law ($\dot{\gamma}^n$) plastic viscosity, where the value of n depends on whether the interfaces are no slip or stress-free (Cohen-Addad et al. 2013). The interplay between shear and deformability is also key to the elastohydrodynamic model of Seth et al. (2011). This model considers soft elastic particles closely packed in a Newtonian fluid. Interparticle lubrication forces induce deformations that depend on $\dot{\gamma}$, which then leads to a $\dot{\gamma}^{1/2}$ viscous term. In addition to foams and concentrated emulsions, this model may be relevant for microgels, in agreement with experimental data (Seth et al. 2011). A different theory envisions zones in the material trapped in the minima of an energy landscape; when the material is sheared, these zones deform elastically until jumps to a new minimum become possible, thus relaxing their stress in a plastic event (e.g., Barrat & Lemaître 2011, Mansard & Colin 2012). In this framework, local viscous dissipation is omitted, although it must play a role in the kinetics of stress relaxation. The stress is purely elastic, and a finite shear rate prevents full stress relaxation between plastic events, leading to the rate dependence of stress. Recent work also shows that, because plastic events are elastically coupled, a single event can trigger entire avalanches (Barrat & Lemaître 2011). Such dynamics requires detailed visualization at the particle scale in experiments and simulations before it can be incorporated into theories.

3.5. Thixotropy

Although several yield-stress fluids behave similarly to the Herschel-Bulkley paradigm (see Section 3.2), a great many others deviate from this ideal rheology. Thixotropy, in particular,

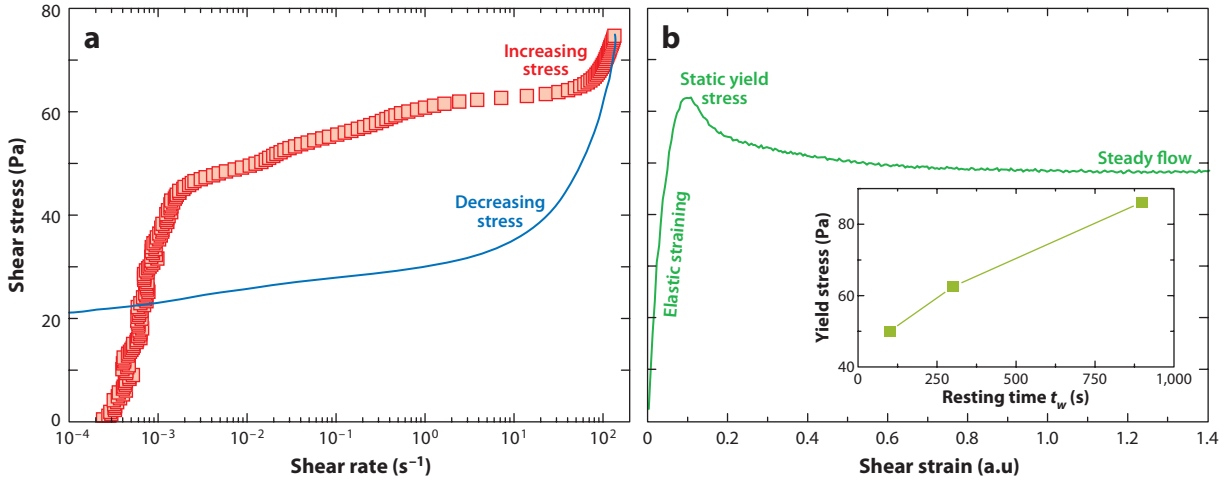

Figure 4

Rheometry of a bentonite suspension. (*a*) A controlled stress ramp showing a thixotropic loop. The red squares represent the data for increasing stress, and the blue line represents decreasing stress. (*b*) A test with an imposed shear rate of $\dot{\gamma} = 10^{-2}$ s^{-1}. (*Inset*) The static yield stress versus resting time. Data taken from Ovarlez & Chateau (2008).

characterizes many yield-stress fluids, including muds, paints, and food products such as ketchup and mayonnaise (Coussot 2005, Mewis & Wagner 2012). Thixotropy leads to history-dependent rheology, as illustrated in **Figure 4*a***.

Thixotropy implies that the static yield stress τ_{y_s} increases with the resting time and is potentially much higher than the dynamic yield stress τ_{y_d} (**Figure 4*b***) (Coussot 2005, Mewis & Wagner 2012, Ovarlez & Chateau 2008). The termination of flow at τ_{y_d} is also very abrupt, with the destructuration suddenly unable to keep pace with the healing of the microstructure. Thus, steady flows quickly brake to rest when the stress falls below the dynamic yield stress τ_{y_d}, with the shear rate jumping discontinuously from finite values $\dot{\gamma} \geq \dot{\gamma}_c$ to zero. The sudden flow switches at the critical stresses, τ_{y_s} and τ_{y_d}, have been termed viscosity bifurcations (Coussot et al. 2002a, Moller et al. 2006). Importantly, these bifurcations imply that there is a range of shear rates $0 < \dot{\gamma} < \dot{\gamma}_c$ for which steady flows are unattainable; if a rheological test sets a macroscopic shear rate within this range, $0 < \dot{\gamma} < \dot{\gamma}_c$, the spatially homogeneous flow unstably breaks up into shear bands (see Section 3.3) (Ovarlez et al. 2009).

The hysteretic behavior of thixotropic fluids plays a major role in fresh concrete casting (Roussel 2011) and the pumping of drilling mud. In the pipelining of waxy crude oils, thixotropy can be problematic after an unanticipated shutdown, requiring enhanced pressure gradients to restart flow. The sudden failure and surprisingly long runout of quick-clay avalanches have also been attributed to thixotropy (Khaldoun et al. 2009).

Thixotropic behavior is typically modeled by making the material parameters of a standard constitutive model depend on an additional variable representing the microstructure (Coussot 2007, Mewis & Wagner 2012). That variable is then usually taken to satisfy an evolution equation containing terms representing structuration and destructuration. When the evolution equation predicts that the material does not stop aging if the shear rate or stress is too low, and if the viscosity diverges for fully structured fluid, an effective yield stress then emerges, even if the constitutive law is taken to be purely viscous. Moreover, flow terminates at a critical shear rate.

Critical shear rate ($\dot{\gamma}_c$): intrinsic property characterizing yielding in thixotropic materials, besides the yield stress; steady homogeneous flow is impossible below $\dot{\gamma}_c$

This is a drastic change of perspective in comparison with the Bingham model and its variants, for which the yield stress is a material parameter of the constitutive behavior. Consistent with the alternative perspective, thixotropic suspensions have been shown to display a purely viscous behavior (with nonmeasurable elasticity) during flow: Solid-like elastic behavior emerges only when flow halts (Ovarlez & Chateau 2008). By contrast, various simple yield-stress fluids have been found to have the same elastic properties in both their solid-like and liquid-like regimes (Benmouffok-Benbelkacem et al. 2010).

3.6. The Shape of the Yield Surface in Stress Space

A rather different consideration for a yield-stress fluid relates to the way in which the material yields under different types of stresses. For example, does the material yield in extension or compression in the same way as that in shear? If so, the force required to pull a coin up from the surface of a layer of mud would be the same as that required to push it into the layer or make the coin rotate. In granular media, yielding is quite different under compression and extension because of the short-range elastic forces that prevent grains from squeezing together at the microscopic level yet present no barrier to pulling them apart.

From the perspective of plasticity theory, any dependence of the yield condition on the stress configuration can be taken into account using the three invariants of the stress tensor (Prager & Hodge 1951). Most generally, the yield criterion can be expressed as a functional relation between these invariants. The von Mises condition used in the Bingham model is just one special case. By contrast, soil mechanicians often use the Mohr-Coulomb condition for granular media. A question that is typically unasked is whether rheological data are more consistent with a yield criterion that is different from the von Mises condition, or if the flow dynamics predicted by a model depends on the yield condition.

Squeeze flow testers are popular devices for compressional rheometry (e.g., Engmann et al. 2005), and measurements of yield stress do seem to correspond to equivalent measurements under shear for some materials in accord with the von Mises condition, once one removes the confounding effect of slip and other problems (Rabideau et al. 2009). Ovarlez et al. (2010) developed a rheometer combining both shear and compression and also found the von Mises criterion to adequately describe yielding in various materials (see **Figure 5**). Similar agreement is found for the tensile failure of pendant drops (**Figure 5**) (German & Bertola 2010a). Any flow involving the displacement of an object in a yield-stress fluid in fact can be seen as a test of the yield criterion, and practical conditions for sedimentation are consistent with the von Mises criterion (see Section 4.3). Finally, theoretical models of glassy materials predict a yield criterion close to von Mises's (Brader et al. 2009). Thus, the von Mises criterion does appear to be appropriate for yield-stress fluids, although the wide range of types of viscoplastic materials undoubtedly will present exceptions to this rule. Interestingly, the same cannot be said of the nonlinear viscous term: The thinning of the viscosity found in shear is not observed in pinching viscoplastic filaments (Aytouna et al. 2013, German & Bertola 2010a).

4. APPLICATIONS IN NATURAL AND ENGINEERING SCIENCES

Given the vast array of different materials that could be considered viscoplastic, it is hardly surprising that applications span several fields. Ancey (2007) reviewed notable geophysical applications, and Mitsoulis (2007) summarized many industrial applications and simulation studies. Here we describe a few application areas that are either topical or unusual, focusing on how a yield stress imposes a key control on the problem or how its manipulation is critical.

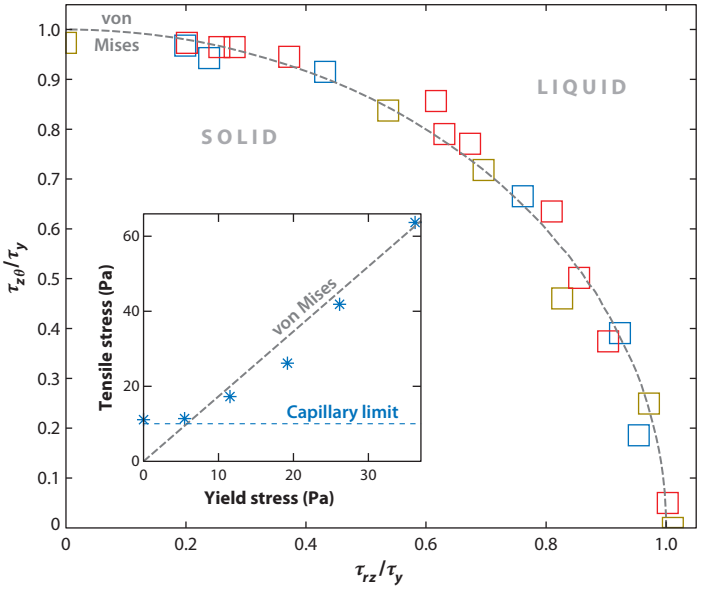

Figure 5

Squeeze (τ_{rz}) versus rotational ($\tau_{z\theta}$) shear stress at yield for two concentrated emulsions (*blue and red squares*) and a Carbopol gel (*dark yellow squares*), each scaled by the yield stress τ_y measured in simple shear. The gray dashed line is the von Mises criterion. Data taken from Ovarlez et al. (2010). (*Inset*) The tensile stress for failure in extension against τ_y, along with the von Mises criterion ($\sqrt{3}\tau_y$), for pendant drops of Carbopol. Data taken from German & Bertola (2010a).

4.1. Control and Actuation by Yield Stresses

Multilayer flows of viscous fluids suffer interfacial instabilities even at low Reynolds numbers, leading to phenomena that plague efforts to lubricate pipelines or produce layered coextrusions. For multilayer viscoplastic flows, interfacial instabilities occur in much the same way when fluids are yielded at the interface (Pinarbasi & Liakopoulos 1995). In contrast, if plugs are maintained at the interface, this surface cannot deform, and the interfacial instability can be suppressed entirely (see Section 2.4) (Frigaard 2001; Hormozi & Frigaard 2012; Moyers-Gonzalez et al. 2004, 2010). The resulting enhancement of flow stability suggests potentially important applications of viscoplastic lubrication, as well as robust methods of droplet encapsulation or control of fluid morphology.

A different category of flows involves smart fluids, meaning in the current context that the yield stress can be controlled in a useful way on the timescale of the flow. Electro- and magnetorheological fluids are one example, often simplistically modeled as viscoplastic fluids with the yield stress dependent on the strength of the applied field. Although fascinating fluids, the detailed flow dynamics is not often studied because the majority of applications exploit the rapid development of large yield stresses in an on/off mode. Interesting recent applications include the control of adhesion of an object to a surface with an intervening magnetorheological fluid (Ewoldt et al. 2011, Lira & Miranda 2009).

Yield stresses can also be manipulated thermally or chemically, suggesting the intriguing possibility of exploiting viscoplastic rheology to activate or terminate flow in a wide variety of ways. For example, Burghelea et al. (2007) used chemical reactions to activate a yield stress near an interface in order to improve the efficiency of fluid displacement. Thermal actuation may be possible with

suspensions of particles grafted with PNIPAM (Crassous et al. 2008), within which the particulate phase swells, depending on temperature, so the material can be above or below the critical volume fraction for a glass transition.

4.2. Free-Surface Flows and Slumps

In free-surface flows, the yield stress ensures that motion eventually grinds to a halt. The shape of the final deposit therefore reflects the yield stress, a notion that underscores two simple rheometers: the slump test (used to gauge the quality of concrete) and the Bostwick consistometer (from the food processing industry).

In the slump test, a fixed volume of fluid is poured from a container and then left to flow to rest; the final height or diameter of the deposit is used to estimate the yield stress (e.g., Roussel 2011). For the Bostwick consistometer, which essentially conducts a viscoplastic dambreak experiment, the sudden removal of a gate in a channel allows the fluid to slump down that conduit; the B_{30} measurement is the distance traveled after 30 s. No direct inference of the yield stress from B_{30} in principle is feasible unless the fluid has slumped close to its final state, as otherwise one cannot disentangle the nonlinear viscous behavior. However, little effort is usually made to relate B_{30} to the material constants of a rheological model; according to the US FDA, the classification of tomato puree as ketchup is dictated purely by its B_{30} measurement.

Viscoplastic gravity currents can be explored using thin-film asymptotics (e.g., Ancey et al. 2012, Balmforth et al. 2006), numerical simulation (Vola et al. 2004), and laboratory experiments (Ancey et al. 2012, Chambon et al. 2008, Cochard & Ancey 2008). Thin-film asymptotics furnishes analytical predictions for the final shape in the shallow limit: For an axisymmetrical deposit on a horizontal plane, the depth is given by

$$h(r) = \sqrt{\frac{2\tau_Y}{\rho g}(R - r)} \tag{4}$$

at radius r, where R is the maximum radius, and g and ρ denote gravity and the fluid density, respectively (e.g., Balmforth et al. 2006). If V is the fluid volume, the yield stress follows as

$$\tau_Y = \frac{\rho g V^2}{128\pi^2 R^5}. \tag{5}$$

Figure 2*b* shows a slump test conducted with Carbopol, together with a more controlled experiment in which the fluid is slowly pumped through a tube onto a plexiglass plate with a roughened surface (to remove the effects of slip; see Section 5). For both deposits, the estimate given in Equation 5 implies a yield stress of approximately 50 Pa. This is somewhat higher than that inferred from rheometry, which is approximately 30 Pa (see **Figure 2*a***), suggesting a problem with the shallow approximation.

Constructions of the final state for planar slumps on inclined planes that avoid the shallow approximation have been worked out based on plasticity theory (Dubash et al. 2008). However, the plasticity solution may not provide the correct final state for an initial-value problem, and the results still do not compare particularly favorably with experiments. Most theory is also confined to Stokes flow. Faster flows demand the inclusion of inertia, which is problematic in shallow-flow theories, viscous and non-Newtonian fluids alike, because the vertical flow structure no longer factors out of the problem. The first steps have been taken toward shallow viscoplastic flow theories with inertia (Fernandez-Nieto et al. 2010, Ionescu 2013), but further work is required to demonstrate their reliability and usefulness. Analysis of the viscoplastic version of the classical dambreak problem therefore remains incomplete.

Other applications include geophysical hazards such as mudslides, lava flows, avalanches, and debris flows (e.g., Ancey 2007, Griffiths 2000) and the damping of water waves by a muddy bottom (Chan & Liu 2009). In engineering, tailing deposits in the mining industry are sometimes emplaced as gravity currents and have the awkward feature of flowing further than expected (Simms et al. 2011). This could result from a poor measurement of the material's yield stress, rather than any fluid mechanical effect, or thixotropy (see Section 3.5). However, the material is also a sedimenting multiphase suspension.

4.3. Sedimentation and Suspensions

A key feature of sedimentation in viscoplastic fluids is that the yield stress can prevent settling. As shown theoretically (Beris et al. 1985) and confirmed experimentally (Tabuteau et al. 2007), a single sphere of diameter d in an infinite yield-stress fluid does not settle if

$$\frac{\tau_y}{\Delta\rho g d} \geq \frac{1}{21}, \tag{6}$$

where $\Delta\rho$ is the density difference between the fluid and the particles. The critical ratio of τ_y to the driving buoyancy stress $\Delta\rho g d$ in Equation 6 corresponds to the plastic limit (see Section 2.2). Similar limits have been determined for circular and elliptical cylinders (Deglo de Besses et al. 2003, Mitsoulis 2004, Putz & Frigaard 2010, Tokpavi et al. 2008) and bubbles (Tsamopoulos et al. 2008). The driving force in Equation 6 need not be buoyancy. Madani et al. (2010) used this principle as the basis of a novel particle fractionation technique, with the driving acceleration coming from the rotation of a centrifuge (see **Figure 1**). The control of the rotation rate and yield stress allows for the sensitive fractionation of particles based on size or density.

Once Equation 6 is violated, the sphere begins to move, and various computational and experimental studies have sought to determine the resulting drag coefficient (Beaulne & Mitsoulis 1997, Blackery & Mitsoulis 1997, Deglo de Besses et al. 2004, Liu et al. 2002, Sikorski et al. 2009, Tabuteau et al. 2007). Unlike viscous sedimentation, the flow becomes localized to the vicinity of the sphere because the stress exerted by the sphere on the fluid decays with distance (Beris et al. 1985). Crucially, this eliminates any Stokes paradox and limits the effect of boundaries (features that carry over to other viscoplastic flows). Nevertheless, recent experiments of particles falling in Carbopol reveal discrepancies with theory, highlighting nonideal properties of this material (Putz et al. 2008, Tokpavi et al. 2009b).

Proceeding beyond a single sphere, our understanding of the dynamics of multiple particles suspended in yield-stress fluids is still in its infancy, despite an increasing interest driven by many industrial applications. For example, for fresh concrete, one wants the material to remain homogeneous at rest, but the heavier constituent particles may settle, a problem that can be avoided by employing a cement paste with sufficient static yield stress (Roussel 2011), which may imply tailoring its thixotropy. Likewise, the continued conveyance of relatively large particles suspended in slurries and drilling mud is important in disposing of mine tailings and clearing oil wells. In hydraulic fracturing, particles transported into fractures by yield-stress fluid help to prop up and maintain the conduit once fracturing ends and withdrawal begins. In other industries, bubbles take the place of particles and may be desirable (hair gel and shampoo manufacturers sell by volume, bubbles included).

Although recent computations have used increasingly exotic combinations of particles (e.g., Liu et al. 2003, Tokpavi et al. 2009a, Yu & Wachs 2007), we have yet to arrive at a scale-able mechanical understanding. Unlike Newtonian fluids, the viscoplastic Stokes equations are not linear, so superposition principles fail. Thus, the foundations of microhydrodynamics (resistance

tensors and so forth) have not developed for viscoplastic fluids, and it is unclear whether the viscoplastic version of Stokesian dynamics computations will ever be feasible.

Alternatively, there have been recent advances in incorporating local dynamics into continuum-level closures for viscoplastic suspensions. Newtonian suspensions are often characterized by making the viscosity increase with the volume fraction (as in the Krieger-Dougherty or Einstein-Roscoe relations). In viscoplastic suspensions, a similar viscosification occurs, but one must also include shear-thinning effects on the local scale because particle crowding tends to locally magnify shear rates, leading to a compensating decrease in viscosity. The overall effect of suspended particles or bubbles on bulk viscosity and yield stress has been evaluated both theoretically and experimentally (Chateau et al. 2008, Kogan et al. 2013, Mahaut et al. 2008), and we now have a characterization of rheological properties according to the volume fraction and properties of the interstitial fluid.

An often underappreciated feature of suspensions of this kind is that particle settling may be critically influenced by macroscopic flow. For example, settling occurs in flow even when Equation 6 is not violated because the macroscopic stress has already exceeded the yield stress, so there is no further resistance to prevent sedimentation (Ovarlez et al. 2012). Even in the macroscopic plugs, the combination of ambient stress and buoyancy may lead to local breaches of the yield stress and sedimentation. Thus, when viscoplastic suspensions are pipelined (e.g., mined tailings or drilled cuttings), the simple notion that rigid plugs magically carry the particulate is conceptually wrong.

4.4. Biological Problems

A number of common biological materials can be considered to be viscoplastic, including mucus, which plays an important role in many biological processes. For snails and slugs, mucus is suggested to be pivotal in allowing both adhesion and locomotion (Denny 1981, Pegler & Balmforth 2013); these locomotors create displacement waves that propagate forward along the underside of their feet (see **Figure 1**). The waves, which translate the organism forward, are interspersed with immobile regions that are stuck to the underlying surface by the mucus yield stress. The waves exert sufficient force to overcome that stress and transport the locomotor forward wave by wave. Snail and slug mucus is also thixotropic (Ewoldt et al. 2007); the ramifications for adhesive locomotion have not yet been quantified, although mucus rheology may have been optimized for this strategy by evolution.

Limpets and other marine organisms use mucus to anchor themselves against ambient water flow. Importantly, the mucus must occasionally release its adhesion to allow the creature to move, and there is evidence suggesting that chemical secretions are used to manipulate the mucus properties (Smith 2002). In other words, limpets may chemically actuate a yield stress to control adhesion.

For other locomotion problems, a yield stress may be the problem rather than the solution: Worms must burrow through mud and peristaltically pump soil through their bodies; microorganisms swim through complex biological fluids. In this situation, the yield stress likely impedes motion (Pegler & Balmforth 2013), leading one to wonder what strategies the organism has developed to move most effectively through or above viscoplastic fluid [optimal strategies for moving over granular layers are currently fashionable (e.g., Ding et al. 2010)]. Such problems have received little attention, and even the simplest models of a swimming microorganism, Taylor's classical waving sheet and corkscrew, currently have no viscoplastic counterpart.

Mucus is used in very different settings in humans. This material lines our lungs and is exploited to remove foreign particles and waste (e.g., Grotberg 2001). The role of viscoplastic rheology in

TURBULENCE AND MIXING IN VISCOPLASTIC FLUIDS

For sufficiently fast flows, the yield stress cannot prevent the transition to turbulence. Phenomenological rules predicting transition have been compared with energy stability theory (Nouar & Frigaard 2001), and there is a broad notion that yield stresses retard transition until the Reynolds stresses are sufficient to yield the fluid (Guzel et al. 2009). Thereafter, only shear thinning remains important (Esmael et al. 2010) and has been identified as the origin of some interesting coherent structures in turbulent viscoplastic shear flows (Esmael & Nouar 2008, López-Carranza et al. 2012). When Reynolds stresses are not sufficient to yield the fluid everywhere, plug zones can provide barriers to mixing and transport. This is also true of many industrial mixers, in which dead zones surround yielded flows, or caverns as they have been called, although an increase in power consumption is needed to limit their extent (Arratia et al. 2006, Savreux et al. 2007).

pulmonary transport, sneezing, and coughing is not often considered (Basser et al. 1989), counter to one's everyday experience (especially after a cold). Are the solid stresses of the mucus exploited in key ways? Is mucus rheology important to removing phlegm, snot, and the like? The critical effect of a yield stress has been studied in other physiological problems such as drug delivery with gels (Tasoglu et al. 2011) and in related cleaning or fouling problems in very different contexts (e.g., Taghavi et al. 2012).

5. TO YIELD OR NOT TO YIELD, AND OTHER POINTS OF CONCLUSION

A key thread through the preceding discussion is the relevance of a yield stress to the application. However, most real fluids are far from idealized, and one may question whether it is worthwhile to face the additional complications introduced by an idealized yield-stress model or if it is better to change the rheology at the outset. In many applications, the purist's approach may not be the most cost-effective. Nevertheless, the improving characterization of real fluids demands the improvement of a model's sophistication.

A related issue regards timescales and the degree of subyield deformation. Other non-Newtonian fluid models are available to represent material behavior in different physical regimes. When the characteristic timescale of the dynamics is relatively short, for example, viscoelasticity can be more important than idealized yield-stress behavior. Mucus, for instance, is often represented as a viscoelastic solid in the biological literature rather than as a yield-stress fluid. One should be sensitively aware of the prevailing physical conditions before selecting a rheological model. Nevertheless, elaborate models with a multitude of material constants are available to bridge the gap between various constitutive laws (e.g., Saramito 2009, Thompson & de Souza Mendes 2012).

Finally, it would be remiss not to summarize some of the other important advances, connections, and open questions that are not mentioned in detail above. Viscoplastic constitutive laws are closely related to recently proposed friction laws for dense granular flow (Forterre & Pouliquen 2008), and less fluid-like geophysical hazards are closely related to shallow granular flows. Turbulence and mixing in viscoplastic fluids are critically important in many applications (see the sidebar). Surface tension drives many viscous flows on smaller spatial scales; the viscoplastic analogs have received only superficial attention, despite the potentially interesting and rich competition between capillarity and the yield stress (e.g., de Bruyn et al. 2002; German & Bertola 2010a,b; Lavrenteva

& Nir 2010). Recently, it has been fashionable to study the sculpting action of capillary forces and fluid flow on elastic surfaces, or elastocapillarity; can one replace the elastic surface by a yield-stress fluid in viscoplastocapillarity?

Another important practical problem only touched upon above is slip: Yield stresses are underestimated (or even fail to be measured) when there is slip (see **Figure 2*a***). This unsavory feature of viscoplastic fluid dynamics arises from the appearance of a lubricating layer of relatively dilute fluid adjacent to a moving boundary. The dilution of the wall layer could have several origins, ranging from electrostatic forces to shear-induced particle migration; often the origin is subtle and rarely fully understood.

FUTURE ISSUES

1. Future progress in viscoplastic flow computations must combine the continued improvement of core numerical methods with increasingly challenging simulations.
2. To address the deficiencies of idealized yield-stress models, researchers must adapt numerical schemes to use more sophisticated rheological models.
3. A standardization of model constitutive laws is needed to take into account thixotropy, subyield elasticity, and other microscale effects, while avoiding a multitude of fitting parameters.
4. We need a better understanding of the nature of the creep flow below the yield stress.
5. The nonlinear viscous behavior (shear thinning) under different stress conditions (shear versus extension or compression) should be examined.
6. Interfacial and multilayer viscoplastic flows should be explored experimentally and theoretically, and the interplay between yield stress and surface tension should be studied.
7. Turbulent flow in viscoplastic fluids should be explored more deeply, including direct numerical simulation and related tools.
8. Energy stability methods and weakly nonlinear theory for viscoplastic fluids should be developed, along with linear stability analysis of further viscoplastic counterparts to classical hydrodynamic instabilities, perhaps all embedded within a variational framework.

DISCLOSURE STATEMENT

The authors are not aware of any biases that might be perceived as affecting the objectivity of this review.

LITERATURE CITED

Adachi K, Yoshioka N. 1973. On creeping flow of a visco-plastic fluid past a circular cylinder. *Chem. Eng. Sci.* 28:215–26

Ancey C. 2007. Plasticity and geophysical flows. *J. Non-Newton. Fluid Mech.* 142:4–35

Ancey C, Andreini N, Epely-Chauvin G. 2012. Viscoplastic dambreak waves: review of simple computational approaches and comparison with experiments. *Adv. Water Resour.* 46:79–91

Arratia PE, Kukura J, Lacombe J, Muzzio FJ. 2006. Mixing of shear-thinning fluids with yield stress in stirred tanks. *AIChE J.* 52:2310–22

Aytouna M, Paredes J, Shahidzadeh-Bonn N, Moulinet S, Wagner C, et al. 2013. Drop formation in non-Newtonian fluids. *Phys. Rev. Lett.* 110:034501

Balmforth NJ, Craster RV, Rust AC, Sassi R. 2006. Viscoplastic flow over an inclined surface. *J. Non-Newton. Fluid Mech.* 139:103–27
Balmforth NJ, Dubash N, Slim A. 2010. Extensional dynamics of viscoplastic filaments II. Drips and bridges. *J. Non-Newton. Fluid Mech.* 165:1147–60
Balmforth NJ, Hewitt IJ. 2013. Viscoplastic sheets and threads. *J. Non-Newton. Fluid Mech.* 193:28–42
Balmforth NJ, Liu JJ. 2004. Roll waves in mud. *J. Fluid Mech.* 519:33–54
Balmforth NJ, Rust AC. 2009. Weakly nonlinear viscoplastic convection. *J. Non-Newton. Fluid Mech.* 158:36–45
Barnes H. 1999. The yield stress—a review or '$\pi\alpha\nu\tau\alpha\rho\epsilon\iota$'—everything flows? *J. Non-Newton. Fluid Mech.* 81:133–78
Barnes HA, Walters K. 1985. The yield stress myth? *Rheol. Acta* 24:323–26
Barral Q, Ovarlez G, Chateau X, Boujlel J, Rabideau B, Coussot P. 2010. Adhesion of yield stress fluids. *Soft Matter* 6:1343–51
Barrat J-L, Lemaître A. 2011. Heterogeneities in amorphous systems under shear. In *Dynamical Heterogeneities in Glasses, Colloids, and Granular Media*, ed. L Berthier, G Biroli, J-P Bouchaud, L Cipelletti, W van Saarloos, pp. 264–97. New York: Oxford Univ. Press
Basser PA, McMahon TJ, Griffith P. 1989. The mechanism of mucus clearance in cough. *Trans. ASME* 111:288–97
Beaulne M, Mitsoulis E. 1997. Creeping motion of a sphere in tubes filled with Herschel-Bulkley fluids. *J. Non-Newton. Fluid Mech.* 72:55–71
Benmouffok-Benbelkacem G, Caton F, Baravian C, Skali-Lami S. 2010. Non-linear viscoelasticity and temporal behavior of typical yield stress fluids: Carbopol, xanthan and ketchup. *Rheol. Acta* 49:305–14
Beris AN, Tsamopoulos JA, Armstrong RC, Brown RA. 1985. Creeping motion of a sphere through a Bingham plastic. *J. Fluid Mech.* 158:219–44
Besseling R, Isa L, Ballesta P, Petekidis G, Cates ME, Poon WCK. 2010. Shear banding and flow-concentration coupling in colloidal glasses. *Phys. Rev. Lett.* 105:268301
Besseling R, Weeks E, Schofield A, Poon W. 2007. Three-dimensional imaging of colloidal glasses under steady shear. *Phys. Rev. Lett.* 99:028301
Blackery J, Mitsoulis E. 1997. Creeping motion of a sphere in tubes filled with a Bingham plastic material. *J. Non-Newton. Fluid Mech.* 70:59–77
Bonn D, Rodts S, Groenink M, Rafai S, Shahidzadeh-Bonn N, Coussot P. 2008. Some applications of magnetic resonance imaging in fluid mechanics: complex flows and complex fluids. *Annu. Rev. Fluid Mech.* 40:209–33
Brader JM, Voigtmann T, Fuchs M, Larson RG, Cates ME. 2009. Glass rheology: from mode-coupling theory to a dynamical yield criterion. *Proc. Natl. Acad. Sci. USA* 106:15186–91
Burghelea T, Wielage-Burchard K, Frigaard I, Martinez DM, Feng J. 2007. A novel low inertia shear flow instability triggered by a chemical reaction. *Phys. Fluids* 19:083102
Burgos GR, Alexandrou AN, Entov V. 1999. On the determination of yield surfaces in Herschel-Bulkley fluids. *J. Rheol.* 43:463–83
Caton F, Baravian C. 2008. Plastic behavior of some yield stress fluids: from creep to long-time yield. *Rheol. Acta* 47:601–7
Chambon G, Ghemmour A, Laigle D. 2008. Gravity-driven surges of a viscoplastic fluid: an experimental study. *J. Non-Newton. Fluid Mech.* 158:54–62
Chan IC, Liu LF. 2009. Responses of Bingham-plastic muddy seabed to a surface solitary wave. *J. Fluid Mech.* 618:155–80
Chateau X, Ovarlez G, Trung KL. 2008. Homogenization approach to the behavior of suspensions of non-colloidal particles in yield stress fluids. *J. Rheol.* 52:489–506
Chaudhuri P, Berthier L, Bocquet L. 2012. Inhomogeneous shear flows in soft jammed materials with tunable attractive forces. *Phys. Rev. E* 85:021503
Cheddadi I, Saramito P, Graner F. 2012. Steady Couette flows of elastoviscoplastic fluids are nonunique. *J. Rheol.* 56:213–39
Cochard S, Ancey C. 2008. Experimental investigation of the spreading of viscoplastic fluids on inclined planes. *J. Non-Newton. Fluid Mech.* 158:73–84

Cohen-Addad S, Höhler R, Khidas Y. 2004. Origin of the slow linear viscoelastic response of aqueous foams. *Phys. Rev. Lett.* 93:028302
Cohen-Addad S, Höhler R, Pitois O. 2013. Flow in foams and flowing foams. *Annu. Rev. Fluid Mech.* 45:241–67
Coussot P. 2005. *Rheometry of Pastes, Suspensions and Granular Materials*. New York: Wiley
Coussot P. 2007. Rheophysics of pastes: a review of microscopic modelling approaches. *Soft Matter* 3:528–40
Coussot P, Nguyen QD, Huynh HT, Bonn D. 2002a. Viscosity bifurcation in thixotropic, yielding fluids. *J. Rheol.* 46:573–89
Coussot P, Raynaud JS, Bertrand F, Moucheront P, Guilbaud JP, et al. 2002b. Coexistence of liquid and solid phases in flowing soft-glassy materials. *Phys. Rev. Lett.* 88:218301
Coussot P, Tabuteau H, Chateau X, Tocquer L, Ovarlez G. 2006. Aging and solid or liquid behavior in pastes. *J. Rheol.* 50:975–94
Coussot P, Tocquer L, Lanos C, Ovarlez G. 2009. Macroscopic versus local rheology of yield stress fluids. *J. Non-Newton. Fluid Mech.* 158:85–90
Crassous JJ, Siebenburger M, Ballauff M, Drechsler M, Hajnal D. 2008. Shear stresses of colloidal dispersions at the glass transition in equilibrium and in flow. *J. Chem. Phys.* 128:204902
Da Cruz F, Chevoir F, Bonn D, Coussot P. 2002. Viscosity bifurcation in granular materials, foams, and emulsions. *Phys. Rev. E* 66:051305
de Bruyn JR, Habdas P, Kim S. 2002. Fingering instability of a sheet of yield-stress fluid. *Phys. Rev. E* 66:031504
Deglo de Besses B, Magnin A, Jay P. 2003. Viscoplastic flow around a cylinder in an infinite medium. *J. Non-Newton. Fluid Mech.* 115:27–49
Deglo de Besses B, Magnin A, Jay P. 2004. Sphere drag in a viscoplastic fluid. *AIChE J.* 50:2627–29
Denny MW. 1981. A quantitative model for the adhesive locomotion of the terrestrial slug *Ariolimax columbianus*. *J. Exp. Biol.* 91:195–217
Derksen JJ. 2013. Simulations of mobilization of Bingham layers in a turbulently agitated tank. *J. Non-Newton. Fluid Mech.* 191:25–34
Dimakopoulos Y, Pavlidis M, Tsamopoulos J. 2013. Steady bubble rise in Herschel-Bulkley fluids and comparison of predictions via the augmented Lagrangian method with those via the Papanastasiou model. *J. Non-Newton. Fluid Mech.* 200:34–51
Ding Y, Gravish N, Li C, Maladen RD, Mazouchova N, et al. 2010. Comparative studies reveal principles of movement on and within granular media. In *IMA Workshop on Locomotion: Natural Locomotion in Fluids and on Surfaces*, ed. S Childress, A Hosoi, WW Schultz, ZJ Wang, pp. 281–92. IMA Vol. Math. Appl. 155. New York: Springer
Divoux T, Barentin C, Manneville S. 2011. From stress-induced fluidization processes to Herschel-Bulkley behaviour in simple yield stress fluids. *Soft Matter* 7:8409–18
Dollet B, Graner F. 2007. Two-dimensional flow of foam around a circular obstacle: local measurements of elasticity, plasticity and flow. *J. Fluid Mech.* 585:181–211
Dubash N, Balmforth NJ, Slim AC, Cochard S. 2008. What is the final shape of a viscoplastic slump? *J. Non-Newton. Fluid Mech.* 158:91–100
Dubash N, Frigaard IA. 2004. Conditions for static bubbles in visco-plastic fluids. *Phys. Fluids* 16:4319–30
Duvaut G, Lions JL. 1976. Rigid visco-plastic Bingham fluid. In *Inequalities in Mechanics and Physics*, ed. G Duvant, JL Lions, pp. 279–327. Transl. CW John. Grundlehren Math. Wiss. 219. New York: Springer-Verlag (From German)
Engmann J, Servais C, Burbidge AS. 2005. Squeeze flow theory and applications to rheometry: a review. *J. Non-Newton. Fluid Mech.* 132:1–27
Esmael A, Nouar C. 2008. Transitional flow of a yield-stress fluid in a pipe: evidence of a robust coherent structure. *Phys. Rev. E* 77:057302
Esmael A, Nouar C, Lefèvre A, Kabouya N. 2010. Transitional flow of a non-Newtonian fluid in a pipe: experimental evidence of weak turbulence induced by shear-thinning behavior. *Phys. Fluids* 22:101701
Ewoldt RH, Clasen C, Hosoi AE, McKinley GH. 2007. Rheological fingerprinting of gastropod pedal mucus and bioinspired complex fluids for adhesive locomotion. *Soft Matter* 3:634–43
Ewoldt RH, Tourkine P, McKinley GH, Hosoi AE. 2011. Controllable adhesion using field-activated fluids. *Phys. Fluids* 23:073104

Fall A, Bertrand F, Ovarlez G, Bonn D. 2009. Yield stress and shear banding in granular suspensions. *Phys. Rev. Lett.* 103:178301
Fall A, Lemaître A, Bertrand F, Bonn D, Ovarlez G. 2010. Continuous and discontinuous shear thickening in granular suspension. *Phys. Rev. Lett.* 105:268303
Fernandez-Nieto ED, Noble P, Vila JP. 2010. Shallow water equations for non-Newtonian fluids. *J. Non-Newton. Fluid* 165:712–32
Forterre Y, Pouliquen O. 2008. Flows of dense granular media. *Annu. Rev. Fluid Mech.* 40:1–24
Frigaard IA. 2001. Super-stable parallel flows of multiple visco-plastic fluids. *J. Non-Newton. Fluid Mech.* 100:49–76
Frigaard IA, Howison SD, Sobey IJ. 1994. On the stability of Poiseuille flow of a Bingham fluid. *J. Fluid Mech.* 263:133–50
Frigaard IA, Ngwa G, Scherzer O. 2003. On effective stopping time selection for visco-plastic nonlinear BV diffusion filters. *SIAM J. Appl. Math.* 63:1911–34
Frigaard IA, Nouar C. 2005. On the use of viscosity regularisation methods for visco-plastic fluid flow computation. *J. Non-Newton. Fluid Mech.* 127:1–26
Frigaard IA, Ryan D. 2004. Flow of a visco-plastic fluid in a channel of slowly varying width. *J. Non-Newton. Fluid Mech.* 123:67–83
Georgievskii DV. 2011. Stability of Bingham flows: from the earliest works of A.A. Ilyushin to the present. *J. Eng. Math.* 78:9–17
German G, Bertola V. 2010a. Formation of viscoplastic drops by capillary breakup. *Phys. Fluids* 22:033101
German G, Bertola V. 2010b. The free-fall of viscoplastic drops. *J. Non-Newton. Fluid Mech.* 165:825–28
Glowinski R, Lions JL, Tremolieres R. 1981. *Numerical Analysis of Variational Inequalities*. Amsterdam: North-Holland
Glowinski R, Wachs A. 2011. On the numerical simulation of viscoplastic fluid flow. In *Handbook of Numerical Analysis*, Vol. 16, ed. R Glowinski, J Xu, pp. 483–717. Amsterdam: Elsevier
Goyon J, Colin A, Ovarlez G, Ajdari A, Bocquet L. 2008. Spatial cooperativity in soft glassy flows. *Nature* 454:84–87
Griffiths RW. 2000. Dynamics of lava flows. *Annu. Rev. Fluid Mech.* 32:477–518
Grotberg JB. 2001. Respiratory fluid mechanics and transport processes. *Annu. Rev. Biomed. Eng.* 3:421–57
Guzel B, Burghelea T, Frigaard IA, Martinez DM. 2009. Observation of laminar-turbulent transition of yield stress fluid in Hagen-Poiseuille flow. *J. Fluid Mech.* 627:97–128
Hewitt IJ, Balmforth NJ. 2012. Viscoplastic lubrication theory with application to bearings and the washboard instability of a planing plate. *J. Non-Newton. Fluid Mech.* 169:74–90
Hormozi S, Frigaard IA. 2012. Nonlinear stability of a visco-plastically lubricated viscoelastic fluid flow. *J. Non-Newton. Fluid Mech.* 169:61–73
Hormozi S, Wielage-Burchard K, Frigaard IA. 2011. Entry, start up and stability effects in visco-plastically lubricated pipe flows. *J. Fluid Mech.* 673:432–67
Ionescu IR. 2013. Viscoplastic shallow flow equations with topography. *J. Non-Newton. Fluid Mech.* 193:116–28
Kamrin K, Mahadevan L. 2012. Soft catenaries. *J. Fluid Mech.* 691:165–77
Karapetsas G, Tsamopoulos J. 2006. Transient squeeze flow of viscoplastic materials. *J. Non-Newton. Fluid Mech.* 133:35–56
Katgert G, Tighe BP, Möbius ME, van Hecke M. 2010. Couette flow of two-dimensional foams. *Europhys. Lett.* 90:54002
Khaldoun A, Moller P, Fall A, Wegdam G, de Leeuw B, et al. 2009. Quick clay and landslides of clayey soils. *Phys. Rev. Lett.* 103:188301
Kogan M, Ducloué L, Goyon J, Chateau X, Pitois O, Ovarlez G. 2013. Mixtures of foam and paste: suspensions of bubbles in yield stress fluids. *Rheol. Acta* 52:237–53
Landry MP, Frigaard IA, Martinez DM. 2006. Stability and instability of Taylor-Couette flows of a Bingham fluid. *J. Fluid Mech.* 560:321–53
Lavrenteva OM, Nir A. 2010. Viscoplastic flows with free boundaries and interfaces. *Rev. Chem. Eng.* 26:149–70
Lipscomb GG, Denn MM. 1984. Flow of Bingham fluids in complex geometries. *J. Non-Newton. Fluid Mech.* 14:337–46

Lira SA, Miranda JA. 2009. Field-controlled adhesion in confined magnetorheological fluids. *Phys. Rev. E* 80:046313
Liu BT, Muller SJ, Denn MM. 2002. Convergence of a regularization method for creeping flow of a Bingham material about a rigid sphere. *J. Non-Newton. Fluid Mech.* 102:179–91
Liu BT, Muller SJ, Denn M. 2003. Interactions of two rigid spheres translating collinearly in creeping flow in a Bingham material. *J. Non-Newton. Fluid Mech.* 113:49–67
Liu A, Nagel S. 2001. *Jamming and Rheology: Constrained Dynamics on Microscopic and Macroscopic Scales*. London: Taylor & Francis
López-Carranza SN, Jenny M, Nouar C. 2012. Pipe flow of shear-thinning fluids. *C. R. Méc.* 340:602–18
Luu LH, Forterre Y. 2009. Drop impact of yield-stress fluids. *J. Fluid Mech.* 632:301–27
Madani A, Storey S, Olson JA, Frigaard IA, Salmela J, Martinez DM. 2010. Fractionation of non-Brownian rod-like particle suspensions in a viscoplastic fluid. *Chem. Eng. Sci.* 65:1762–72
Mahaut F, Chateau X, Coussot P, Ovarlez G. 2008. Yield stress and elastic modulus of suspensions of non-colloidal particles in yield stress fluids. *J. Rheol.* 52:287–313
Manneville S. 2008. Recent experimental probes of shear banding. *Rheol. Acta* 47:301–18
Mansard V, Colin A. 2012. Local and non local rheology of concentrated particles. *Soft Matter* 8:4025–43
Masschaele K, Fransaer J, Vermant J. 2009. Direct visualization of yielding in model two-dimensional colloidal gels subjected to shear flow. *J. Rheol.* 53:1437–60
Matson GP, Hogg AJ. 2007. Two-dimensional dambreaks of Herschel-Bulkley fluids: the approach to the arrested state. *J. Non-Newton. Fluid Mech.* 142:79–94
Métivier C, Nouar C, Brancher JP. 2005. Linear stability involving the Bingham model when the yield stress approaches zero. *Phys. Fluids* 17:104106
Métivier C, Nouar C, Brancher JP. 2010. Weakly nonlinear dynamics of thermoconvective instability involving viscoplastic fluids. *J. Fluid Mech.* 660:316–53
Mewis J, Wagner NJ. 2012. *Colloidal Suspension Rheology*. Cambridge, UK: Cambridge Univ. Press
Mitsoulis E. 2004. On creeping drag flow of a viscoplastic fluid past a circular cylinder: wall effects. *Chem. Eng. Sci.* 59:789–800
Mitsoulis E. 2007. Flows of viscoplastic materials: models and computations. *Rheol. Rev.* 2007:135–78
Moller PCF, Fall A, Bonn D. 2009. Origin of apparent viscosity in yield stress fluids below yielding. *Europhys. Lett.* 87:38004
Moller PCF, Mewis J, Bonn D. 2006. Yield stress and thixotropy: on the difficulty of measuring yield stresses in practice. *Soft Matter* 2:274–83
Moller PCF, Rodts S, Michels MAJ, Bonn D. 2008. Shear banding and yield stress in soft glassy materials. *Phys. Rev. E* 77:041507
Mossolov PP, Miasnikov VP. 1965. Variational methods in the theory of the fluidity of a viscous plastic medium. *J. Mech. Appl. Math.* 29:468–92
Moyers-Gonzalez MA, Frigaard IA, Nouar C. 2004. Nonlinear stability of a visco-plastically lubricated viscous shear flow. *J. Fluid Mech.* 506:117–46
Moyers-Gonzalez MA, Frigaard IA, Nouar C. 2010. Stable two-layer flows at all Re: visco-plastic lubrication of shear-thinning and viscoelastic fluids. *J. Non-Newton. Fluid Mech.* 165:1578–87
Muravleva L, Muravleva E, Georgiou GC, Mitsoulis E. 2010. Numerical simulations of cessation flows of a Bingham plastic with the augmented Lagrangian method. *J. Non-Newton. Fluid Mech.* 165:544–50
Nouar C, Kabouya N, Dusek J, Mamou M. 2007. Modal and non-modal linear stability of the plane Bingham-Poiseuille flow. *J. Fluid Mech.* 577:211–39
Nouar C, Frigaard IA. 2001. Nonlinear stability of Poiseuille flow of a Bingham fluid: theoretical results and comparison with phenomenological criteria. *J. Non-Newton. Fluid Mech.* 100:127–49
Oppong FK, de Bruyn JR. 2011. Microrheology and jamming in a yield-stress fluid. *Rheol. Acta* 50:317–26
Ovarlez G, Barral Q, Coussot P. 2010. Three-dimensional jamming and flows of soft glassy materials. *Nat. Mater.* 9:115–19
Ovarlez G, Bertrand F, Coussot P, Chateau X. 2012. Shear-induced sedimentation in yield stress fluids. *J. Non-Newton. Fluid Mech.* 177:19–28
Ovarlez G, Chateau X. 2008. Influence of shear stress applied during flow stoppage and rest period on the mechanical properties of thixotropic suspensions. *Phys. Rev. E* 77:061403

Ovarlez G, Cohen-Addad S, Krishan K, Goyon J, Coussot P. 2013. On the existence of a simple yield stress fluid behavior. *J. Non-Newton. Fluid Mech.* 193:68–79
Ovarlez G, Rodts S, Chateau X, Coussot P. 2009. Phenomenology and physical origin of shear localization and shear banding in complex fluids. *Rheol. Acta* 48:831–44
Pegler SS, Balmforth NJ. 2013. Locomotion over a layer of viscoplastic fluid. *J. Fluid Mech.* 727:1–29
Peng J, Zhu KQ. 2004. Linear stability of Bingham fluids in spiral Couette flow. *J. Fluid Mech.* 512:21–46
Piau JM. 2007. Carbopol gels: elastoviscoplastic and slippery glasses made of individual swollen sponges; meso- and macroscopic properties, constitutive equations and scaling laws. *J. Non-Newton. Fluid Mech.* 144:1–29
Pignon F, Magnin A, Piau J. 1998. Thixotropic behavior of clay dispersions: combinations of scattering and rheometric techniques. *J. Rheol.* 42:1349–73
Pinarbasi A, Liakopoulos A. 1995. Stability of two-layer Poiseuille flow of Carreau-Yasuda and Bingham-like fluids. *J. Non-Newton. Fluid Mech.* 57:227–41
Pinkus O, Sternlicht B. 1961. *Theory of Hydrodynamic Lubrication*. New York: McGraw-Hill
Prager W. 1954. On slow visco-plastic flow. In *Studies in Mathematics and Mechanics: Presented to Richard von Mises by Colleagues, Friends, and Pupils*. New York: Academic
Prager W, Hodge PG. 1951. *Theory of Perfectly Plastic Solids*. New York: Wiley
Putz A, Burghelea T, Martinez DM, Frigaard IA. 2008. Settling of an isolated spherical particle in a yield stress shear thinning fluid. *Phys. Fluids* 20:033102
Putz A, Frigaard IA. 2010. Creeping flow around particles in a Bingham fluid. *J. Non-Newton. Fluid Mech.* 165:263–80
Putz A, Frigaard IA, Martinez DM. 2009. On the lubrication paradox and the use of regularisation methods for lubrication flows. *J. Non-Newton. Fluid Mech.* 163:62–77
Rabideau BD, Lanos C, Coussot P. 2009. An investigation of squeeze flow as a viable technique for determining the yield stress. *Rheol. Acta* 48:517–26
Rahmani Y, Habibi M, Javadi A, Bonn D. 2011. Coiling of yield stress fluids. *Phys. Rev. E* 83:056327
Roquet N, Saramito P. 2003. An adaptive finite element method for Bingham fluid flows around a cylinder. *Comput. Methods Appl. Mech. Eng.* 192:3317–41
Roussel N, ed. 2011. *Understanding the Rheology of Concrete*. Cambridge: Woodhead
Salmon JB, Bécu L, Manneville S, Colin A. 2003. Towards local rheology of emulsions under Couette flow using dynamic light scattering. *Eur. Phys. J. E* 10:209–21
Saramito P. 2009. A new elastoviscoplastic model based on the Herschel-Bulkley viscoplastic model. *J. Non-Newton. Fluid Mech.* 158:154–61
Savreux F, Jay P, Magnin A. 2007. Viscoplastic fluid mixing in a rotating tank. *Chem. Eng. Sci.* 62:2290–301
Schall P, van Hecke M. 2010. Shear bands in matter with granularity. *Annu. Rev. Fluid Mech.* 42:67–88
Seth JR, Mohan L, Locatelli-Champagne C, Cloitre M, Bonnecaze RT. 2011. A micromechanical model to predict the flow of soft particle glasses. *Nat. Mater.* 10:838–43
Sherwood JD, Durban D. 1998. Squeeze-flow of a Herschel-Bulkley fluid. *J. Non-Newton. Fluid Mech.* 77:115–21
Sikorski D, Tabuteau H, de Bruyn JR. 2009. Motion and shape of bubbles rising through a yield-stress fluid. *J. Non-Newton. Fluid Mech.* 159:10–16
Simms P, Williams MPA, Fitton TG, McPhail G. 2011. Beaching angles and evolution of stack geometry for thickened tailings: a review. In *Paste 2011: Proc. 14th Int. Semin. Paste Thick. Tailings*, ed. RJ Jewell, AB Fourie, pp. 323–38. Perth: Aust. Cent. Geomech.
Smith AM. 2002. The structure and function of adhesive gels from invertebrates. *Integr. Comp. Biol.* 42:1164–71
Szabo P, Hassager O. 1992. Flow of viscoplastic fluids in eccentric annular geometries. *J. Non-Newton. Fluid Mech.* 45:149–69
Tabuteau H, Coussot P, de Bruyn JR. 2007. Drag force on a sphere in steady motion through a yield-stress fluid. *J. Rheol.* 51:125–37
Taghavi SM, Alba K, Moyers-Gonzalez M, Frigaard IA. 2012. Incomplete fluid-fluid displacement of yield stress fluids in near-horizontal pipes: experiments and theory. *J. Non-Newton. Fluid Mech.* 167:59–74
Tasoglu S, Park SC, Peters JJ, Katz DF, Szeri AJ. 2011. The consequences of yield stress on deployment of a non-Newtonian anti-HIV microbicide gel. *J. Non-Newton. Fluid Mech.* 166:1116–22

Thompson RL, de Souza Mendes P. 2012. A critical overview of elasto-viscoplastic thixotropic modelling. *J. Non-Newton. Fluid Mech.* 187:8–15

Tokpavi DL, Jay P, Magnin A. 2009a. Interaction between two circular cylinders in slow flow of Bingham viscoplastic fluid. *J. Non-Newton. Fluid Mech.* 157:175–87

Tokpavi DL, Jay P, Magnin A, Jossic L. 2009b. Experimental study of the very slow flow of a yield stress fluid around a circular cylinder. *J. Non-Newton. Fluid Mech.* 164:35–44

Tokpavi DL, Magnin A, Jay P. 2008. Very slow flow of Bingham viscoplastic fluid around a circular cylinder. *J. Non-Newton. Fluid Mech.* 154:65–76

Tsamopoulos J, Dimakopoulos Y, Chatzidai N, Karapetsas G, Pavlidis M. 2008. Steady bubble rise and deformation in Newtonian and viscoplastic fluids and conditions for bubble entrapment. *J. Fluid Mech.* 601:123–64

Vikansky A. 2008. Lattice-Boltzmann method for yield-stress liquids. *J. Non-Newton. Fluid Mech.* 155:95–100

Vinay G, Wachs A, Agassant JF. 2006. Numerical simulation of weakly compressible Bingham flows: the restart of pipeline flows of waxy crude oils. *J. Non-Newton. Fluid Mech.* 136:93–105

Vola D, Babik F, Latché JC. 2004. On a numerical strategy to compute gravity currents of non-Newtonian fluids. *J. Comput. Phys.* 201:397–420

Walton IC, Bittleston SH. 1991. The axial flow of a Bingham plastic in a narrow eccentric annulus. *J. Fluid Mech.* 222:39–60

Yu Z, Wachs A. 2007. A fictitious domain method for dynamic simulation of particle sedimentation in Bingham fluids. *J. Non-Newton. Fluid Mech.* 145:78–91

Zhang JY, Frigaard IA, Vola D. 2006. Yield stress effects on Rayleigh-Bénard convection. *J. Fluid Mech.* 566:389–419

RELATED RESOURCES

Many other applications and recent contributions are included in four special journal issues (*Journal of Non-Newtonian Fluid Mechanics*, volumes 142, 158, and 193, and *Rheologica Acta*, volume 50), each drawn from an ongoing series of workshops on viscoplastic fluids.

Annual Review of
Fluid Mechanics

Volume 46, 2014

Contents

Indexes

Errata

An online log of corrections to *Annual Review of Fluid Mechanics* articles may be found at http://fluid.annualreviews.org/errata.shtml